ARTICLE IN PRESS

Corrosion Science xxx (xxxx) xxx–xxx

Contents lists available at ScienceDirect

Corrosion Science

journal homepage: www.elsevier.com/locate/corsci

A study on corrosion behavior of friction stir welded and tungsten inert gas welded AA2014 aluminium alloy

Sunil Sinhmar*, Dheerendra Kumar Dwivedi

Mechanical & Industrial Engineering Department, Indian Institute of Technology Roorkee, Roorkee 247667, Uttarakhand, India

ARTICLE INFO

Keywords:
Aluminium
Welding
Pitting corrosion
Polarization
EIS

ABSTRACT

The present study comprises the comparison of the electrochemical behavior of friction stir weld (FSW) joint and tungsten inert gas (TIG) weld joint of AA2014 using immersion test, potentiodynamic polarization test and electrochemical impedance spectroscopy (EIS). Weld thermal cycles and microhardness were correlated with corrosion behavior of the weld joints. TIG weld joint showed lower corrosion resistance than FSW joint. Heat affected zone was the most corrosion susceptible region in both type of weld joints. Optical microscopy, FESEM, TEM and XRD analysis were performed to discuss the corrosion behavior in light of the microstructure.

1. Introduction

2xxx series heat treatable aluminium alloys have copper as their major alloying element. AA2014 aluminium alloy is a widely used alloy of this series owing to its high strength to weight ratio. AA2014 aluminium alloy is preferably used in aerospace industry. Welding of this alloy is difficult due to the tendency of welding defects formation. Fusion welding of Al–Cu alloys mainly produces porosity and cracks [1]. Solid state welding like friction stir welding can produce sound weld joint of AA2014 aluminium alloy at optimized process parameters.

Although, the fusion welding of aluminium alloy is a big challenge, however, tungsten inert gas welding has been used for last many years. Double sided TIG welding was used for joining of thick aluminium alloy plates [2]. Friction stir welding is a new welding technique as compared to the TIG welding and it was invented in 1991 at 'The welding institute (TWI)' in UK [3]. Friction stir welding uses a non-consumable rotating tool plunged into abutting surfaces of the plates to be welded. The movement of the tool causes plastic deformation which results in to the welding. Temperature rise is due to the combined effect of the frictional heat produced by shoulder and plastic deformation caused by pin of the tool. The temperature rise in FSW remains below the melting point of the alloy, whereas TIG welding causes melting of the material in fusion zone. Different zones formed during the FSW are nugget zone (NZ) – region which stirred by pin and experiences recrystallization and plastic deformation, thermo-mechanical affected zone (TMAZ) – region which experience only plastic deformation, heat affected zone (HAZ) – region which experience only change in microstructure due to thermal cycle, and base metal (Fig. 1a). Similarly, zones formed during the TIG welding are fusion zone (FZ), HAZ and base metal (Fig. 1b).

Corrosion resistance of AA2014 aluminium alloy is very poor and most of the time it is susceptible to the pitting corrosion. Non-uniformity in the microstructure of this alloy is the major reason for poor corrosion resistance. The chemical composition of AA2014 is given in Table 1. AA2014 mainly contains θ phase (Al_2Cu) within the matrix and at the grain boundaries. Welding results into the change in microstructure and creates various zones having different grain sizes and precipitates. These variations reduce corrosion resistance of the alloy.

Corrosion behavior of the friction stir welded AA2A14 aluminium alloys was investigated in EXCO (exfoliation corrosion) solution using various electrochemical measurements [4]. Authors studied the effect of immersion time and different phases on the corrosion behavior of the alloy and found that the corrosion attack was increasing with the time. Water cooled friction stir welding was used to suppress the corrosion attack on the AA2014 aluminium alloy [5]. Authors reported that the formation of Al_2Cu precipitate was responsible for accelerating the corrosion reaction. Non-uniform distribution of $MgZn_2$ was responsible for the localized intergranular corrosion of thermo-mechanical affected zone of friction stir welded AA7108 [6]. A network of intergranular precipitates was found to be responsible for severe corrosion in heat affected zone of AA2024 FSW joint [7]. Potentiodynamic polarization and EIS (electrochemical impedance spectroscopy) corrosion tests were performed to investigate the corrosion behavior of FSW joint of thick plates of 2219-O aluminium alloy and it was found that the presence of Cu in coarse intermetallics was responsible for poor corrosion resistance [8]. EIS study was performed on the friction stir processed/welded aluminium alloys and it was found that the second phase particles lowered the corrosion resistance of the alloy [9,10]. Comparative study of the corrosion behavior of FSW joint and TIG weld joint was

* Corresponding author.
E-mail address: sun25.dme2014@iitr.ac.in (S. Sinhmar).

https://doi.org/10.1016/j.corsci.2018.01.012
Received 22 August 2017; Received in revised form 9 January 2018; Accepted 18 January 2018

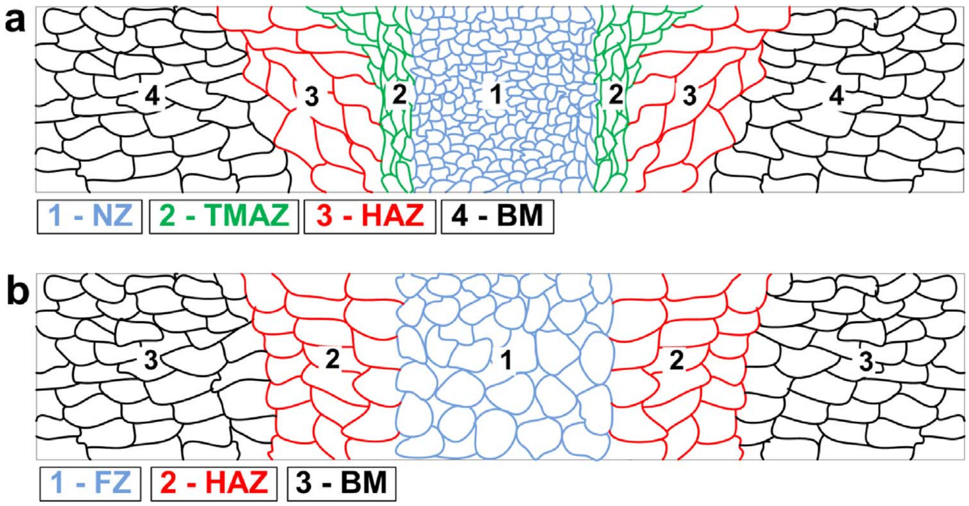

Fig. 1. Schematic of (a) FSW, and (b) TIG weld joint cross section showing different zones formed during welding.

Table 1
Chemical composition (wt%) of AA2014.

Alloy	Cu	Si	Fe	Mn	Mg	Zn	Al
AA2014	4.8	0.97	0.7	0.38	0.54	0.25	Balance

performed on AA2024 and AA6061 aluminium alloys and it was found that phase transformation caused by the high heat input during the TIG welding lead to the more corrosion [11,12]. Metal inert gas weld joint of AA6xxx also showed lower corrosion resistance compared to the FSW joint [13]. HAZ was the most corrosion susceptible region in the TIG weld joint of AA2219. It was attributed to the segregation and reversion of second phase (Al_2Cu) along the grain boundary [14].

As the AA2014 is a very important aluminium alloy from the commercial point of view, so it is essential to study the corrosion behavior of this alloy. FSW and TIG welding are the two major joining techniques uses for this alloy. Corrosion behavior of the FSW joint of AA2014 was studied in the literature but same for TIG welding alone and comparative study of FSW and TIG weld joint of AA2014 is not available to the author's knowledge. Although heat input during the welding is a very important factor, but comparative weld thermal cycles for both welding techniques in correlation with corrosion behavior has not been reported. The present study investigates the corrosion behavior of AA2014 correlating with microstructure (including precipitate reversion and coarsening) and weld thermal cycle history.

2. Experimental procedure

As received AA2014-T651 aluminium alloy plates were used for the FSW and TIG welding. Plate dimensions were 70 mm × 27.5 mm × 6 mm and 100 mm × 27.5 mm × 6 mm for FSW and TIG welding, respectively. Abutting surfaces were properly cleaned using acetone before the welding. An indigenous modified vertical milling machine (15 HP) was used for the FSW. Plates were properly clamped in the fixture before starting of the welding. The non consumable tool of 'H13 steel' having a cylindrical threaded pin of Inconel was used for the FSW. Rotational and traverse speeds were 931 rpm and 41 mm/min, respectively. Tool dimensions and friction stir welding parameters are given in Table 2. Axial force (F) during FSW was 3.5 kN and concavity (α) at the shoulder of FSW tool was 5°.

Double sided TIG welding was carried out on 'EWM Triton 180 AC/DC hightec welding' machine without using any filler material. Process parameters used for the TIG welding are given in Table 3. Samples were extracted for various testing and characterization after performing both types of welding. Fig. 2 is showing the plates welded using FSW and TIG

Table 2
Tool dimensions and FSW process parameters.

Tool dimensions				FSW parameters		
Shoulder diameter (mm)	Pin shape	Pin diameter (mm)	Pin length (mm)	Rotational speed (rpm)	Traverse speed (mm/min)	Tool tilt angle (°)
18	Cylindrical (threaded)	M6	5.7	931	41	1.5

Table 3
TIG welding process parameters.

Welding current (A)	Voltage (V)	Welding speed (mm/min)	Shielding gas	Gas flow rate (l/min)
150	12	150	Ar	15

welding along with schematic of the position of thermocouples. Samples from transverse cross-section were polished on SiC papers up to 2000 grit and then followed by rough and fine cloth polishing using heavy magnesium oxide powder slurry. Keller's etchant (2.5 ml of HNO_3, 1.5 ml HCl, 1.0 ml of HF and 95 ml of distilled water) was applied on the polished samples for 25 s to reveal the grain boundaries.

Optical microscopy was performed on Dewinter LT-23B microscope and 'Image J' software was used to calculate the average grain size of each zone of the weld joints. Field emission scanning electron microscopy (FESEM) and energy dispersive X-ray spectroscopy (EDS) were used for micro analysis of elements present in the different phases. X-ray diffraction (XRD) with CuKα radiation was used to analyze the phases of the joints. Transmission electron microscopy (TEM) was used on the electron transparent foils of the joints for profound study. Microhardness study of the both weld joints was performed using Vicker's microhardness tester. Load, dwell time and distance between two consecutive indentations were 100 g, 10 s and 0.5 mm, respectively. The temperature was measured during welding using K-type thermocouples. Thermocouple wires were inserted into the drilled holes of 1.5 mm diameter and 3 mm depth at the bottom side of the plates to be welded. A special backing plate with slots was prepared to accommodate the thermocouple wires. The locations of the holes were kept at 5 mm and 10 mm distance from the weld center line in both the welding techniques. Thermocouple wire was not kept in the center of the weld because the moving pin of the FSW tool and melting in TIG welding could have destroyed the wire.

Corrosion behavior of the upper surface of weld joints obtained